Recent J/ψ results in p+p and Au+Au collisions from STAR

Kaifeng Shen[1,2,*] (for the STAR Collaboration)

[1]Department of Modern Physics, University of Science and Technology of China, Hefei 230026, China
[2]State Key Laboratory of Particle Detection and Electronics, University of Science and Technology of China, Hefei 230026, China

Abstract. In these proceedings, we present the measurements of inclusive J/ψ production at mid-rapidity region ($|y| < 1.0$) in Au+Au collisions at $\sqrt{s_{\rm NN}}$ = 54.4 GeV by the STAR experiment. The dependences of nuclear modification factor ($R_{\rm AA}$) on centrality and transverse momentum (p_T) are presented and compared to model calculations. No significant energy dependence of $R_{\rm AA}$ is found within uncertainties. We also report the distribution of $z(J/\psi) = p_T^{J/\psi}/p_T^{jet}$ and the fraction of J/ψ produced within a charged jet at mid-pseudorapidity ($|\eta| < 0.6$) with kinematic cuts of $p_T^{jet} > 10$ GeV/c and $p_T^{J/\psi} > 5$ GeV/c in p+p collisions at $\sqrt{s} = 500$ GeV. Comparisons to model calculations are presented and physics implications are discussed.

1 Introduction

Heavy quarks (charm and beauty) are ideal probes to study the properties of the Quark-Gluon Plasma (QGP), because they are mainly produced via initial hard partonic scatterings and thus experience the entire evolution of the QGP created in high-energy heavy-ion collisions. Quarkonia are bound states of heavy quarks and their anti-quarks, such as charm-anticharm and bottom-antibottom, and potential holding these bound states could be screened by partons in the QGP [1]. Therefore, the cross-section of quarkonia would be reduced in heavy-ion collisions with respect to those in p+p collisions scaled by the number of binary nucleon-nucleon collisions, $N_{\rm coll}$, at the same energy. Suppression of the J/ψ meson production has been observed in different collision systems at SPS, RHIC, and LHC energies [2–7]. In previous measurements by the STAR Collaboration [5], the collision energy ($\sqrt{s_{\rm NN}}$) dependence of the J/ψ suppression between 39 and 200 GeV was studied and found to be insignificant within uncertainties. In 2017, about ten times more statistics for Au+Au collisions at 54.4 GeV, compared to that used for previous STAR measurement at 62.4 GeV, was collected by the STAR experiment. This will help to understand the collision energy dependence of the J/ψ suppression with improved precision.

The production mechanism of J/ψ mesons involves both perturbative quantum chromodynamics (QCD) process - the production of charm and anti-charm pairs, and nonperturbative QCD process - the evolution of charm and anti-charm pair to a J/ψ. The latter is still not fully understood [8]. The nonrelativistic QCD (NRQCD) factorization formalism is one of the most successful approaches to describe the J/ψ production [9], which parameterizes the

*e-mail: skfwyl@mail.ustc.edu.cn

© The Authors, published by EDP Sciences. This is an open access article distributed under the terms of the Creative Commons Attribution License 4.0 (http://creativecommons.org/licenses/by/4.0/).

nonperturbative hadronization process with long-distance matrix elements (LDMEs). However, there exist significant differences in values of LDMEs extracted by different groups [10]. Measurements of the J/ψ production within a jet are predicated to exhibit strong distinguishing power among different models [11]. LHCb and CMS collaborations have reported their measurements of the J/ψ production within a jet [12, 13]. The observed $z(J/\psi) = p_T^{J/\psi}/p_T^{jet}$ distributions for prompt J/ψ, where $p_T^{J/\psi}$ and p_T^{jet} are the transverse momenta for J/ψ and jet, do not agree with the predictions from PYTHIA 8 [12], but can be well described by LDMEs from fits to high p_T data [14]. Measuring the J/ψ production within a jet at RHIC will provide complementary information on the J/ψ production mechanism.

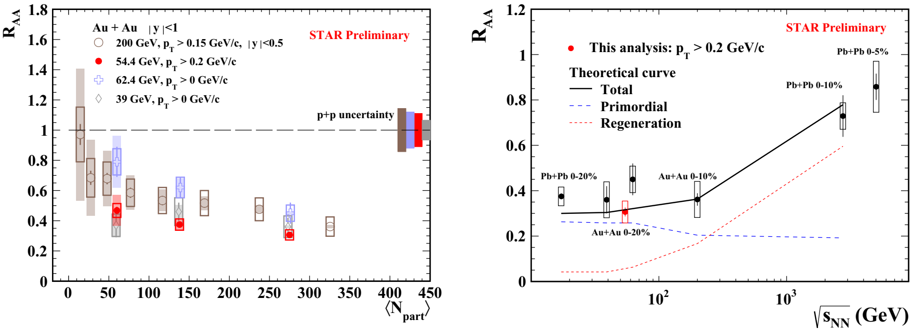

Figure 1: *Left panel*: The R_{AA} of inclusive J/ψ as a function of $\langle N_{\mathrm{part}}\rangle$ in Au+Au collisions at different collision energies at mid-rapidity [5, 6]. The error bars represent the statistical uncertainties. The boxes represent the systematic uncertainties. The shaded bands on the data points indicate the uncertainties from the nuclear overlap function $\langle T_{\mathrm{AA}}\rangle$ [15]. The bands around unity indicate the uncertainties from the p+p baselines. *Right panel*: The R_{AA} of J/ψ as a function of collision energy for central collisions, in comparison with model calculations [16]. The SPS result at $\sqrt{s_{\mathrm{NN}}} = 17.2$ GeV is from [2, 3]; the STAR points at $\sqrt{s_{\mathrm{NN}}} = 39$, 62.4 and 200 GeV are from [5, 6]; the ALICE points at $\sqrt{s_{\mathrm{NN}}} = 2.76$ and 5.02 TeV are from [4, 7]. The error bars represent the statistical uncertainties and the boxes represent the systematic uncertainties, including those from p+p baselines and uncertainties from $\langle T_{\mathrm{AA}}\rangle$.

2 J/ψ production in Au+Au collisions at $\sqrt{s_{\mathrm{NN}}} = 54.4$ GeV

The data sample used in this measurement is 1.3 billion minimum-bias Au+Au events at $\sqrt{s_{\mathrm{NN}}} = 54.4$ GeV collected in 2017 by the STAR experiment. A J/ψ candidate is reconstructed through its decay into an electron-positron pair, and electron candidates are reconstructed and identified using information from the Time Projection Chamber (TPC) [17], Time-of-Flight (TOF) [18], and the Barrel Electromagnetic Calorimeter (BEMC) [19].

The nuclear modification factor, R_{AA}, is defined as follows:

$$R_{\mathrm{AA}} = \frac{1}{\langle T_{\mathrm{AA}}\rangle} \frac{d^2N_{\mathrm{AA}}/dp_T dy}{d^2\sigma_{\mathrm{pp}}^{INEL}/dp_T dy},$$

where $d^2N_{\mathrm{AA}}/dp_T dy$ is the J/ψ yield in A+A collisions and $d^2\sigma_{\mathrm{pp}}^{INEL}/dp_T dy$ is the J/ψ cross section in p+p collisions. The nuclear overlap function is defined as $T_{\mathrm{AA}}(\mathbf{b}) = \int T_{\mathrm{A}}(\mathbf{s})T_{\mathrm{A}}(\mathbf{s} - \mathbf{b})d^2s$, where $T_{\mathrm{A}}(\mathbf{s})$ is the transverse nucleon density and $\mathbf{b}$ is the impact parameter.

The p_T-integrated R_{AA} as a function of the mean number of participants $\langle N_{\mathrm{part}} \rangle$ in Au+Au collisions of different collision energies is shown in the left panel of Fig. 1. Since there are no measurements of inclusive J/ψ cross section available in p+p collisions at 39, 54.4 and 62.4 GeV, the p+p baselines are extracted from interpolations of world data [15]. The p+p baseline at 17.2 GeV is established by the data collected with lighter projectiles [20]; the p+p baseline at 200 GeV is obtained by combining STAR and PHENIX measurements [21, 22]; the p+p baseline at 2.76 TeV is obtained by interpolating the inclusive J/ψ cross-sections at mid-rapidity measured by PHENIX [23], CDF [24] and ALICE [25–27]; the p+p baseline at 5.02 TeV is measured by ALICE [28]. Suppression of the J/ψ production is observed in Au+Au collisions at 54.4 GeV with improved precision compared to previous results at 39 and 62.4 GeV. The right panel of Fig. 1 shows the R_{AA} as a function of collision energy for different collision systems in central collisions. There is no significant energy dependence within uncertainties up to 200 GeV. The solid line is a theoretical calculation of J/ψ R_{AA} from [16], in which the blue dash-dotted line represents the suppressed primordial production due to cold nuclear matter effects (CNM) and dissociation in the QGP medium, while the red dashed line denotes the regeneration contribution. The theoretical calculation is consistent with the observed energy dependence, indicating that the J/ψ production in high-energy heavy-ion collisions is affected by several effects, such as CNM, dissociation in the QGP medium, and regeneration.

Figure 2 shows the J/ψ R_{AA} as a function of p_T at different collision energies (left) and centralities (right). A larger suppression is observed at lower p_T and towards more central collisions.

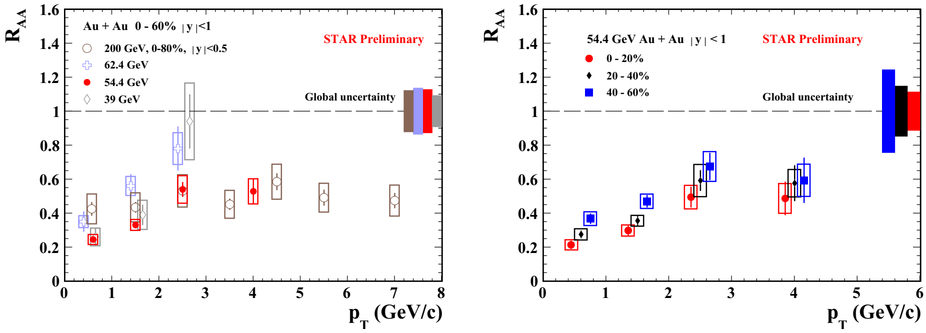

Figure 2: The inclusive J/ψ R_{AA} as a function of p_T in Au+Au collisions [5, 6]. The error bars represent the statistical uncertainties. The boxes represent the systematic uncertainties. The bands around unity indicate the uncertainties from the $\langle T_{\mathrm{AA}} \rangle$ and the p+p baselines.

3 J/ψ production in jets in p+p collisions at $\sqrt{s} = 500$ GeV

The data sample used in this measurement was collected from p+p collisions at $\sqrt{s} = 500$ GeV in 2011 and the integrated luminosity of this sample is 22.1 pb^{-1}. Events are triggered by the BEMC requiring an energy deposition larger than 4.3 GeV in at least one BEMC tower. The J/ψ candidates are reconstructed through their decays into electron-positron pairs, and the electron candidates are reconstructed and identified using information from the TPC and BEMC. The jet reconstruction is performed for events with a J/ψ candidate by clustering the J/ψ candidate with charged particles using the anti-k_T algorithm as implemented in the FASTJET package [30].

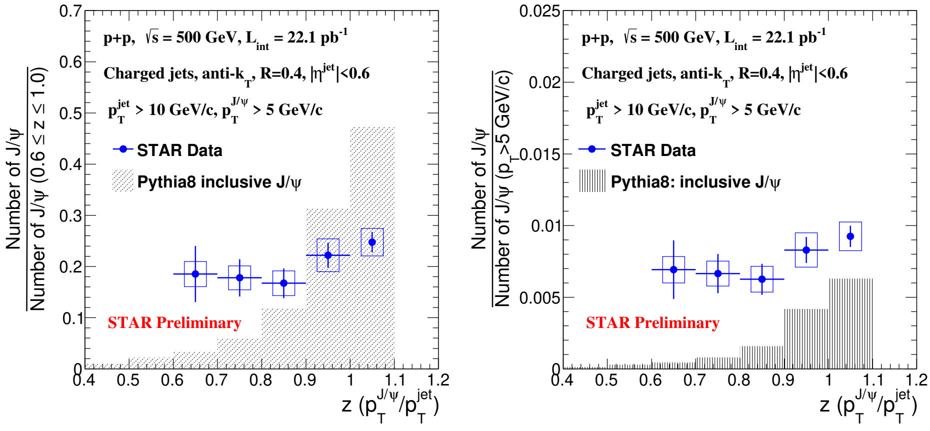

Figure 3: *Left panel*: The z distribution of inclusive J/ψ produced within a jet, normalized by the number of J/ψ with z from 0.6 to 1.0, and compared to prediction from PYTHIA 8 (gray filled histogram). The vertical lines represent statistical uncertainties and the blue boxes display systematic uncertainties. The data point for isolated J/ψ ($z = 1$) is placed at 1.05 for clarity. *Right panel*: The ratio of inclusive J/ψ produced within a jet to the total J/ψ yield [29] as a function of z, compared to PYTHIA 8 prediction.

The left panel of Fig. 3 shows the self-normalized $z(J/\psi) = p_T^{J/\psi}/p_T^{jet}$ distribution for inclusive J/ψ mesons with $p_T^{J/\psi} > 5$ GeV/c produced within a charged jet of $p_T^{jet} > 10$ GeV/c. No significant $z(J/\psi)$ dependence for $z < 1$ is observed within uncertainties. The experimental results are compared to the leading-order NRQCD-based PYTHIA 8 calculation [31], and a different trend is observed in data and PYTHIA prediction. The less isolated production of J/ψ in data than that predicted by PYTHIA 8 is similar to the LHC measurements [12, 13]. The right panel of Fig. 3 shows the ratio of the number of J/ψ within a charged jet for $p_T^{J/\psi}$ > 5 GeV/c and $p_T^{jet} > 10$ GeV/c to the total number of J/ψ with $p_T^{J/\psi} > 5$ GeV/c [29]. The fraction is measured to be 3.7% ± 0.3% (stat.) ± 0.2% (sys.), significantly larger than the PYTHIA 8 predicition.

4 Summary

In this contribution, the recent results on J/ψ production in p+p and Au+Au collisions from STAR are discussed. Newly measured R_{AA} for J/ψ meson at $\sqrt{s_{\mathrm{NN}}} = 54.4$ GeV is shown as a function of $\langle N_{\mathrm{part}} \rangle$ and p_T with improved precision compared to previous measurements at 39 and 62.4 GeV. There is no significant energy dependence of R_{AA} in central collisions from 17.2 to 200 GeV within uncertainties. The first measurement of J/ψ production within a charged jet in p+p collisions at RHIC ($\sqrt{s} = 500$ GeV) is shown and compared to PYTHIA 8 predictions. The J/ψ production is less isolated in data compared to that in PYTHIA 8 and more probable to be produced in jets.

Acknowledgements

This work was funded by the National Natural Science Foundation of China under Grant Nos. 11720101001 and 11775213, Anhui Provincial Natural Science Foundation under Grant Nos. 1908085J02.

References

[1] T. Matsui, H. Satz, Phys. Lett. B **178**, 416 (1986)
[2] L. Kluberg, Eur. Phys. J. C **43**, 145 (2005)
[3] M.C. Abreu et al. (NA50), Phys. Lett. B **477**, 28 (2000)
[4] B.B. Abelev et al. (ALICE), Phys. Lett. B **734**, 314 (2014), `1311.0214`
[5] L. Adamczyk et al. (STAR), Phys. Lett. B **771**, 13 (2017), `1607.07517`
[6] J. Adam et al. (STAR), Phys. Lett. B **797**, 134917 (2019), `1905.13669`
[7] X. Bai (ALICE), Nucl. Phys. A **1005**, 121769 (2021), `2001.11925`
[8] N. Brambilla et al., Eur. Phys. J. C **71**, 1534 (2011), `1010.5827`
[9] Y.Q. Ma, R. Venugopalan, Phys. Rev. Lett. **113**, 192301 (2014), `1408.4075`
[10] J.P. Lansberg, Phys. Rept. **889**, 1 (2020), `1903.09185`
[11] Z.B. Kang, J.W. Qiu, F. Ringer, H. Xing, H. Zhang, Phys. Rev. Lett. **119**, 032001 (2017), `1702.03287`
[12] R. Aaij et al. (LHCb), Phys. Rev. Lett. **118**, 192001 (2017), `1701.05116`
[13] A.M. Sirunyan et al. (CMS), Phys. Lett. B **804**, 135409 (2020), `1910.01686`
[14] R. Bain, L. Dai, A. Leibovich, Y. Makris, T. Mehen, Phys. Rev. Lett. **119**, 032002 (2017), `1702.05525`
[15] W. Zha, B. Huang, R. Ma, L. Ruan, Z. Tang, Z. Xu, C. Yang, Q. Yang, S. Yang, Phys. Rev. C **93**, 024919 (2016), `1506.08985`
[16] X. Zhao, R. Rapp, Phys. Rev. C **82**, 064905 (2010), `1008.5328`
[17] M. Anderson et al., Nucl. Instrum. Meth. A **499**, 659 (2003), `nucl-ex/0301015`
[18] W. Llope, Nuclear Instruments and Methods in Physics Research Section A: Accelerators, Spectrometers, Detectors and Associated Equipment **661**, S110 (2012), x. Workshop on Resistive Plate Chambers and Related Detectors (RPC 2010)
[19] M. Beddo et al. (STAR), Nucl. Instrum. Meth. A **499**, 725 (2003)
[20] M. Abreu, J. Astruc, C. Baglin, A. Baldit, M. Bedjidian, P. Bordalo, A. Bohrani, A. Bussière, P. Busson, J. Castor et al., Physics Letters B **466**, 408 (1999)
[21] J. Adam, L. Adamczyk, J. Adams, J. Adkins, G. Agakishiev, M. Aggarwal, Z. Ahammed, N. Ajitanand, I. Alekseev, D. Anderson et al., Physics Letters B **786**, 87 (2018)
[22] A. Adare, S. Afanasiev, C. Aidala, N.N. Ajitanand, Y. Akiba, H. Al-Bataineh, J. Alexander, K. Aoki, L. Aphecetche, J. Asai et al. (PHENIX Collaboration), Phys. Rev. D **82**, 012001 (2010)
[23] A. Adare, S. Afanasiev, C. Aidala, N.N. Ajitanand, Y. Akiba, H. Al-Bataineh, J. Alexander, A. Al-Jamel, K. Aoki, L. Aphecetche et al. (PHENIX Collaboration), Phys. Rev. Lett. **98**, 232301 (2007)
[24] D. Acosta, J. Adelman, T. Affolder, T. Akimoto, M.G. Albrow, D. Ambrose, S. Amerio, D. Amidei, A. Anastassov, K. Anikeev et al. (CDF Collaboration), Phys. Rev. D **71**, 032001 (2005)

[25] B. Abelev, J. Adam, D. Adamová, A. Adare, M. Aggarwal, G. Aglieri Rinella, A. Agocs, A. Agostinelli, S. Aguilar Salazar, Z. Ahammed et al., Physics Letters B **718**, 295 (2012)

[26] K. Aamodt, A. Abrahantes Quintana, D. Adamová, A. Adare, M. Aggarwal, G. Aglieri Rinella, A. Agocs, A. Agostinelli, S. Aguilar Salazar, Z. Ahammed et al., Physics Letters B **704**, 442 (2011)

[27] K. Aamodt, A. Abrahantes Quintana, D. Adamová, A. Adare, M. Aggarwal, G. Aglieri Rinella, A. Agocs, A. Agostinelli, S. Aguilar Salazar, Z. Ahammed et al., Physics Letters B **718**, 692 (2012)

[28] S. Acharya et al. (ALICE), JHEP **10**, 084 (2019), 1905.07211

[29] J. Adam et al. (STAR), Phys. Rev. D **100**, 052009 (2019), 1905.06075

[30] M. Cacciari, G.P. Salam, G. Soyez, Eur. Phys. J. C **72**, 1896 (2012), 1111.6097

[31] T. Sjostrand, S. Mrenna, P.Z. Skands, Comput. Phys. Commun. **178**, 852 (2008), 0710.3820